

Mössbauer and muon studies of β -(NH₄)₂FeF₅

M. Attenborough, I. Hall, and O. Nikolov

Department of Physics, Oliver Lodge Laboratory, University of Liverpool, Liverpool, L69 3BX, United Kingdom

S. R. Brown

ISIS Facility, Rutherford Appleton Laboratory, Chilton, Didcot, OX11 0QX, United Kingdom

S. F. J. Cox

*ISIS Facility, Rutherford Appleton Laboratory, Chilton, Didcot, OX11 0QX, United Kingdom
and Department of Physics, University College London, Gower Street, London, WC1E 6BT, United Kingdom*

(Received 26 June 1995; revised manuscript received 12 February 1996)

We report variable-temperature Mössbauer and muon spin relaxation (μ SR) studies of the antiferromagnet β -(NH₄)₂FeF₅. The magnetically split Mössbauer spectra from the ordered phase are complex and are fitted with distributions of hyperfine fields. At any particular temperature the distribution falls largely into two groups and these have different mean ordering temperatures of approximately 9.2 and 11.3 K. The μ SR experiments confirm that the ordering is staggered. In the paramagnetic region the μ SR time spectra are oscillatory and characteristic of (FMuF)⁻ ion formation. This signal is attenuated at high temperature, an effect attributed to muon diffusion, and attenuated also at temperatures close to magnetic ordering, an effect attributed to critical fluctuations in the Fe ion spin system. The muons sense the slowing down of the Fe spins by both the direct Fe-Mu interaction and the indirect Fe-¹⁹F-Mu interaction. [S0163-1829(96)00433-X]

I. INTRODUCTION

The nuclear-probe technique of Mössbauer spectroscopy, especially that based on ⁵⁷Fe, has proved to be very effective in the microscopic study of magnetic phenomena. Muon spin rotation or relaxation is also a nuclear-probe technique, in some ways complementary to the Mössbauer method, and has found increasing application in magnetism studies in recent years. In the present work both techniques have been brought to bear on an investigation of the antiferromagnet β -(NH₄)₂FeF₅.

Our work was triggered by the report by Calage *et al.*¹ of a Mössbauer study of the α and β forms of (NH₄)₂FeF₅. The β form showed an apparent two-sextet structure in the Mössbauer spectra below the ordering temperature $T_N \approx 13$ K. It was assumed that the two magnetic hyperfine fields corresponding to these sextets converged to zero at a single ordering temperature between the datapoints at 12 and 14 K although, as pointed out by the authors, this implied a “dramatic” drop in the magnetization curve for the higher-field component. It seemed to us that an alternative, although still rather novel, scenario might be the existence of two ordering temperatures for this material. This possibility was prompted by the case of another NH₄-containing antiferromagnet (NH₄)₂FeCl₅·H₂O. Among the A₂FeX₅·H₂O family (A=alkali or NH₄, X=halogen) this compound is unique in various ways but, for the present, we mention only the existence of two closely spaced heat-capacity cusps² in the region of $T_N \approx 7$ K. Various ⁵⁷Fe Mössbauer spectroscopy measurements³⁻⁵ showed that spectra in the antiferromagnetic region could not be satisfactorily fitted with only one magnetic component and it was suggested by two of us⁵ that the two heat-capacity cusps were associated with two magnetic ordering temperatures. The following questions thus arose:

Does β -(NH₄)₂FeF₅ have more than one ordering temperature? If so, is this attributable in both β -(NH₄)₂FeF₅ and (NH₄)₂FeCl₅·H₂O to the NH₄ ion? In any event, what are the similarities and differences between these two compounds?

Now in Mössbauer spectroscopy the ordering temperature is taken to be that at which the measured magnetic hyperfine field B_{hf} falls to zero on approach from the low-temperature (ordered) side. Ordinarily this operational definition is consistent with determination by other methods. However, because of the apparently unusual behavior of the compound and because the loss of magnetic spectral splitting might in principle be due to some other spin dynamic effect, it seemed important to use also a different technique. For this reason we undertook also a μ SR study of β -(NH₄)₂FeF₅. The μ SR measurements were made at the ISIS Facility of the Rutherford Appleton Laboratory. Schenk⁶ and Cox,⁷ for example, have described how spin-polarized muons may be implanted in a sample and the depolarization measured via the time dependence of the back-forward asymmetry of the positron count from the muon decay. At ISIS the muon pulses are approximately 80 ns wide.⁸ Thus, as the temperature falls below T_N and the internal magnetic field in an ordered material causes the muons to precess with a period of much less than 80 ns, the asymmetry measured with a powder sample drops to one third, this being the polycrystalline average of the static component of the polarization. It is this drop in initial asymmetry that we have used as the signature of magnetic ordering. We show here that our Mössbauer and muon experiments are in excellent agreement on the two-staged nature of the ordering in β -(NH₄)₂FeF₅. We also find differences between the cases of β -(NH₄)₂FeF₅ and (NH₄)₂FeCl₅·H₂O.

In the course of the preliminary μ SR experiments it was found that the asymmetry vs time spectra showed oscillatory

behavior in the paramagnetic region. This was ascribed to the formation of (FMuF)⁻ ions.⁹ In an (FMuF)⁻ ion the muon is electrostatically bonded between two F⁻ ions such that the latter are brought together to a separation of just less than one ionic diameter. The nucleus ¹⁹F is the only naturally occurring fluorine isotope and the ¹⁹F:μ: ¹⁹F coupled system of three spin-1/2 particles gives a distinctive μSR signal. Earlier reports of the (FMuF)⁻ system are given in, for example, Refs. 10–13. We found the (FMuF)⁻ signal to be most pronounced in the 30–100 K temperature range, which presumably implies damping of the signal outside this range. The most likely causes of this damping are critical fluctuations in the Fe ion spin system at low temperature and muon hopping at high temperature. There are, however, several interactions which are candidates for consideration in the overall shaping of the μSR spectra from β-(NH₄)₂FeF₅, so that the problem of interpretation of these spectra is complex. Nevertheless we have endeavored to use the (FMuF)⁻ signal to trace the temperature dependence of the principal muon depolarization mechanisms over a wide temperature range, and this is discussed in Sec. II.

Although the unusual nature of the magnetic ordering of β-(NH₄)₂FeF₅ motivated this work and was the focus of the initial (Mössbauer) experiments, the muon depolarization in the paramagnetic region emerged as a second principal topic and, for presentational purposes, it is more convenient to discuss it first. Thus the Mössbauer data are presented in Sec. III and both principal topics are discussed in Sec. IV.

II. MUON SPIN RELAXATION

A. Experiment

Powder samples of β-(NH₄)₂FeF₅ were prepared as described by Bentrup and Kolditz¹⁴ and Fourquet *et al.*¹⁵ Three samples were prepared, differing only in the baking time in the final (dehydration) stage. Room-temperature XRD spectra of all were as reported by Fourquet *et al.*,¹⁵ the latter reporting the crystal symmetry to be *P*_{nma} and the structure to have kinked chains of trans-linked FeF₆ octahedra running along [010]. In one case we checked that the x-ray spectrum was unchanged by thermal cycling to 4.2 K and back. The μSR and Mössbauer data reported here are almost all from one sample.

The μSR experiments were performed on the EMU instrument at the ISIS Facility. The temperature was varied with an Oxford Instruments continuous helium flow cryostat, regulated by an ITC5 control system, the sample temperature being monitored with a thermometer in close contact with the sample holder. The temperature stability was approximately ±0.01 K for temperatures below 25 K and better than ±0.1 K at higher temperatures. Approximately 80% of the muons were stopped in the 3-cm-diam sample, those falling outside being intercepted by a silver mask whose μSR signal shows negligible depolarization. A typical spectrum contained 15 million events accumulated over approximately an hour. Zero-field (ZF) spectra were recorded as a function of temperature between 4 and 300 K and examples are shown in Fig. 1. The initial asymmetry observed in the paramagnetic region was close to the maximum normally obtained with this particular instrument and this indicates a high diamagnetic fraction for the implanted muons (i.e., no muonium

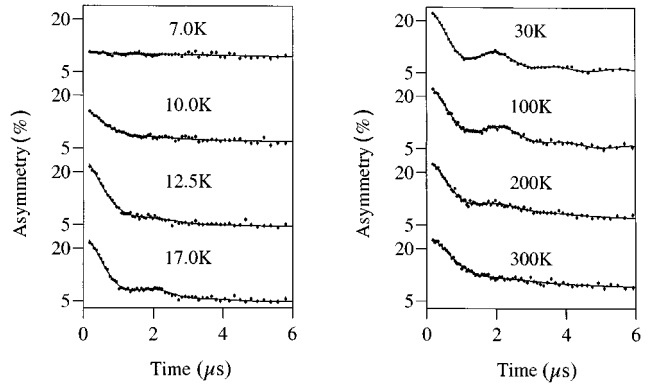


FIG. 1. Some μSR spectra from β-(NH₄)₂FeF₅ at various temperatures.

formation). The oscillatory signal is evident over a wide temperature range. It disappeared on application of a longitudinal field (LF) sufficient to dominate the fields due to the ¹⁹F nuclear spins; this is illustrated in Fig. 2. Below approximately 9 K, where the magnetic ordering is complete, the initial asymmetry is seen to be much reduced and the depolarization rate is small.

B. Analysis

1. Paramagnetic region

The oscillatory depolarization function given by Brewer *et al.*¹¹ for muons in (FMuF)⁻ ions and applied successfully to powder fluoride samples by Noakes *et al.*¹² is

$$g_{\text{FMuF}}(t) = \frac{1}{6} \left[3 + \cos(\sqrt{3}\omega_d t) + \left(1 - \frac{1}{\sqrt{3}}\right) \cos\left\{\frac{3-\sqrt{3}}{2}\omega_d t\right\} + \left(1 + \frac{1}{\sqrt{3}}\right) \cos\left\{\frac{3+\sqrt{3}}{2}\omega_d t\right\} \right] \quad (1)$$

with

$$\hbar\omega_d = \gamma_\mu\gamma_F/r_{F-\mu}^3.$$

Here $\nu_d = \omega_d/2\pi$ is the dipole interaction frequency, γ_μ and γ_F are the muon and ¹⁹F gyromagnetic ratios and $r_{F-\mu}$ is the fluorine-muon separation (≈1.15 Å). The derivation of Eq. (1) assumes that the muon resides half-way between the cen-

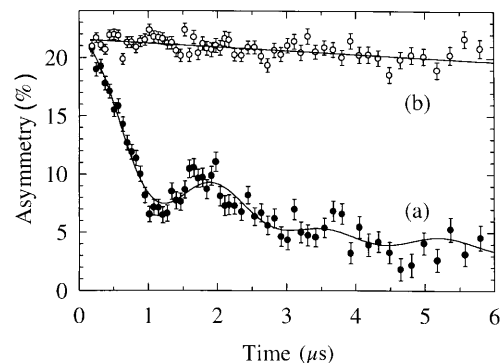


FIG. 2. μSR spectra at 30 K: (a) zero field, (b) 125 G longitudinal field.

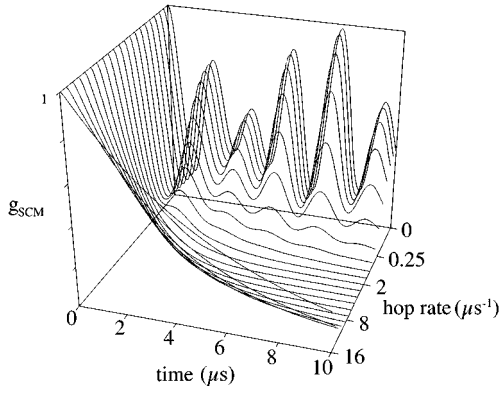


FIG. 3. The $(\text{FMuF})^-$ depolarization function and the effect of muon hop rate according to a strong-collision model.

ters of two very close fluorine ions and that the depolarizing interaction is exclusively that between the muon and the ^{19}F spins. This static relaxation function may be adapted to take account of muon diffusion at higher temperatures in a ‘‘strong-collision model’’¹⁰ (SCM) wherein a muon hops from site to site at a mean frequency ν and it is assumed that there is no correlation between the fields at the muon before and after the jump. The dynamic relaxation function $g_{\text{SCM}}(t)$ may be found by numerical integration of the equation

$$g_{\text{SCM}}(t) = \exp(-\nu t)g_{\text{FMuF}}(t) + \nu \int_0^t g_{\text{SCM}}(t-t') \times \exp(-\nu t')g_{\text{FMuF}}(t')dt'. \quad (2)$$

Although the SCM has been introduced here to describe the situation of sudden changes in muon environment due to muon hopping, it may also be used at low temperatures in the present case when the changes are due to ^{19}F nuclear spin flips induced by critical magnetic fluctuations in the Fe spin system. In the use of Eq. (2) below these cases are distinguished by denoting the muon hop rate by ν_h and the ^{19}F flip rate by ν_F . Also, in setting out the depolarization functions in full, we shall for brevity denote the generation of a SCM function from some basic relaxation function $g(t)$ as in Eq. (2) by the operation

$$g_{\text{SCM}}(t) = \mathcal{S}^\nu\{g(t)\}. \quad (3)$$

The effect of the rate ν on the muon depolarization in an $(\text{FMuF})^-$ system is shown in Fig. 3, a diagram similar to that given earlier by Brewer *et al.*¹⁰

The oscillations in our asymmetry spectra are most visible in the 50-K region. Even there, however, and by comparison with the $\nu=0$ graph in Fig. 3, it is clear that the $(\text{FMuF})^-$ signal is significantly damped. This could be a dynamic effect or it could result from the dephasing of muons precessing in a distribution of static fields due to distant nuclei, i.e., nuclei other than the adjacent ^{19}F nuclei. [Another possibility is that there are two or more muon sites involved in the $(\text{FMuF})^-$ signal with somewhat different $r_{\text{F}-\mu}$. The consequent spread in ω_d would give some attenuation of the oscillatory signal but this is unlikely to be as strong as the observed damping.] Anyway, whatever the cause of the damping and for the purpose only of a preliminary parametrization of our data, we describe it with a stretched expo-

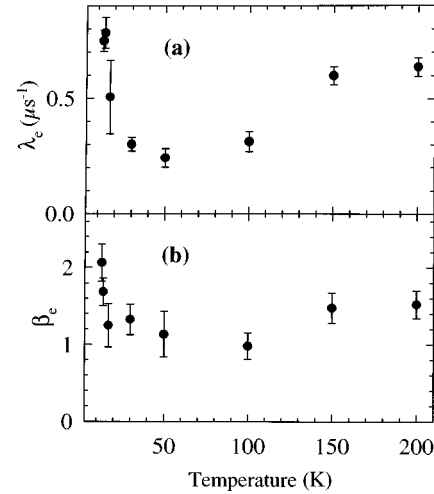


FIG. 4. Fitted values of parameters of the preliminary depolarization function of Eq. (4): (a) λ_e , (b) β_e .

ponential envelope function $\exp(-\lambda_e t)^{\beta_e}$. In addition to the main, oscillatory spectral component it was found necessary to include an underlying component, best fitted by a simple exponential, which is presumably due to muons in an alternative type of site or chemical state. Thus our preliminary depolarization function is

$$g_i(t) = y \exp(-\lambda_e t)^{\beta_e} g_{\text{FMuF}}(t) + (1-y)\exp(-\lambda_u t) \quad (4)$$

and our spectra were fitted to an asymmetry function

$$a(t) = a_s g_i(t) + a_{\text{Ag}}. \quad (5)$$

In Eq. (5) a_s (≈ 0.20) is the initial asymmetry for muons stopped in the sample and a_{Ag} (≈ 0.04) is the constant asymmetry for muons stopped in the silver mask. We found the main-component fraction $y \approx 0.6$ with insignificant variation with temperature and this was borne out also by the final fitting.

Now whereas the above function $g_i(t)$ is supposed to be realistic only in the 50 K region, it is instructive to consider the fitted values of β_e and λ_e over a wider temperature range and these are shown in Fig. 4. It may be seen that in the 50 K region the envelope function is more nearly exponential than Gaussian. It is possible for a distribution of static fields to result in a near-exponential depolarization but the latter does invite the suspicion of a dynamic contribution. However, we may see also in Fig. 4 that the fitted values of λ_e are barely significantly higher at 30 and 100 K than at 50 K. Now the effects of critical fluctuations at low temperature and of muon hopping at high temperature are both expected to be strongly temperature dependent. We may conclude that the attenuation of the $(\text{FMuF})^-$ signal at 50 K is predominantly a static effect. In fact we assume here on that the effect at 50 K is entirely static and in the subsequent analysis we take $\beta_e=1$ and λ_e to be fixed for all temperatures at the value found in this preliminary fitting at 50 K. This assumption may not be totally secure but any error incurred is most unlikely to affect significantly the eventual conclusions about *changes* in the dynamics in the low- and high-temperature regimes.

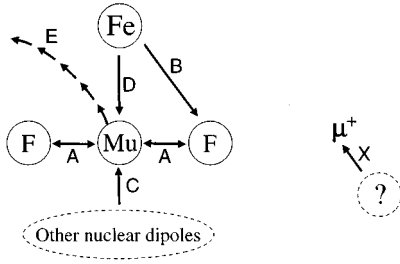


FIG. 5. Interactions and mechanisms involved in the muon depolarization.

We now list and comment on the interactions and processes involved in the more comprehensive analysis applied to the entire temperature range. These are shown diagrammatically in Fig. 5.

(A) The ^{19}F -Mu- ^{19}F coupling, giving rise to the function $g_{\text{FMuF}}(t)$ given in Eq. (1).

(B) The Fe- ^{19}F coupling. This interaction between the Fe ions and the ^{19}F nuclei causes spin flips of the ^{19}F nuclei due to flips of the Fe ion spins. This effect is expected to be pronounced at low temperature due to critical slowing down in the Fe spin system. As already noted, the consequent effect on the muon spectrum may be described by a SCM and the mean ^{19}F flip rate ν_{F} may be related to the mean Fe flip rate ν_{Fe} by the fast relaxation formula

$$\nu_{\text{F}} = \Delta_{\text{F}}^2 / \nu_{\text{Fe}}, \quad (6)$$

where $\Delta_{\text{F}}/\gamma_{\text{F}}$ is the rms field at a ^{19}F nucleus due to the nearby Fe ion. Taking the mean Fe- ^{19}F distance to be approximately 1.9 Å based on the crystallographic data,¹⁵ Δ_{F} is calculated to be 239 μs^{-1} . The fitted rates all have $\nu_{\text{Fe}} \gg \Delta_{\text{F}}$ thus justifying the use of Eq. (6).

(C) The interaction between a muon and distant nuclear dipoles giving rise, as already explained, to a static depolarization function $g_{\text{dist}}(t) = \exp(-\lambda_u t)$. Presumably at very low temperatures this interaction mechanism may also be subject to dynamic effects because of nuclear spin flips arising from critical slowing down in the Fe spin system; however, we defer consideration of this possibility until later.

(D) The Fe-Mu interaction. This may be thought of as the direct interaction between the Fe spins and the muons as distinct from that via B and A. We have taken for this a convenient, analytic, longitudinal relaxation function shown by Keren¹⁶ to be valid for intermediate and fast relaxation rates. Thus

$$g_{\text{Fe-Mu}}(t) = \exp\left[-\frac{2\Delta_{\text{Mu}}^2}{\nu_{\text{Fe}}^2} \{\exp(-\nu_{\text{Fe}} t) - 1 + \nu_{\text{Fe}} t\}\right], \quad (7)$$

where $\Delta_{\text{Mu}}/\gamma_{\mu}$ is the rms field at the muon due to the nearby Fe ion or ions. [It turns out that, for all fitted ν_{Fe} , the even simpler fast-relaxation limit¹⁶ of Eq. (7) would have sufficed.]

(E) The muon hopping.

(X) Whatever causes the underlying component for which $g_{\text{und}}(t) = \exp(-\lambda_u t)$. Although the muons in this component are likely to be subject to at least some of the processes listed above for the main (oscillatory) component, we have insufficient information to deconvolute its relatively simple form.

We now consider the implications for some of these processes of the 125 G LF spectrum at 30 K-[Fig. 2(b)]. This field is sufficient to render inoperative those effects on the muon spectra which depend on nuclear dipole fields at the muon site, i.e., A, B, and C above. In addition, the very slow decline in Fig. 2(b) shows that the depolarization of the underlying component must also have been suppressed by the longitudinal field. It has been suggested^{12,17} that, in other materials containing the $(\text{FMuF})^-$ ion, an underlying component like that found here is due to the delayed formation of muonium with a timescale of the order of a microsecond. However, in the present case this seems unlikely in view of the low decoupling field.

If we suppose that there is no depolarization at all of the underlying component in Fig. 2(b) and we take the muon hop rate $\nu_h = 0$ at 30 K, we can attribute the small depolarization entirely to D above. Indeed the appropriate depolarization function is then

$$g(t) = y g_{\text{Fe-Mu}}(t) + (1-y) \quad (8)$$

and we have used Eq. (8) to fit the 30 K LF spectrum simultaneously with the 30 K ZF spectrum [using $g_p(t)$ below] to estimate the parameter $\Delta_{\text{Mu}} \approx 116 \mu\text{s}^{-1}$. Although this parameter is not particularly well determined, the implication of a field of approximately 1.5 kG at the muon due to the Fe ions is consistent with an external field of this order being required to decouple the muons at 4.5 K (in the magnetically ordered region and where, in the case of a powder sample, the observed depolarization is primarily due to the static field of the direct Fe-Mu interaction.)

We now construct the ZF depolarization function $g_p(t)$ appropriate to the paramagnetic region, bearing in mind our SCM short-hand notation [Eq. (3)] and that, when there are independent depolarization mechanisms, the corresponding functions are to be multiplied. Thus we have

$$g_p(t) = y \mathcal{S}^{\nu_h} \{g_{\text{Fe-Mu}}(\nu_{\text{Fe}}, t) g_{\text{dist}}(t) \mathcal{S}^{\nu_{\text{F}}} \{g_{\text{FMuF}}(\nu_d, t)\}\} + (1-y) g_{\text{und}}(\lambda_u, t), \quad (9)$$

where the parameters appearing explicitly are those which remain to be fitted. Now whereas Eq. (9) formally encapsulates the depolarization algebra applicable to the entire temperature range it is simplified somewhat in application to two temperature regimes. At low temperature ($T < 50$ K) we take $\nu_h = 0$ and then

$$g_p(t) = y g_{\text{Fe-Mu}}(\nu_{\text{Fe}}, t) g_{\text{dist}}(t) \mathcal{S}^{\nu_{\text{F}}} \{g_{\text{FMuF}}(\nu_d, t)\} + (1-y) g_{\text{und}}(\lambda_u, t) \quad (T < 50 \text{ K}) \quad (10)$$

remembering that ν_{Fe} and ν_{F} are not independent but coupled by Eq. (6). At high temperature ($T > 50$ K) we take $\nu_{\text{Fe}} \rightarrow \infty$ so that $g_{\text{Fe-Mu}}(t) \rightarrow 1$ and $\nu_{\text{F}} \rightarrow 0$ and then

$$g_p(t) = y \mathcal{S}^{\nu_h} \{g_{\text{dist}}(t) g_{\text{FMuF}}(\nu_d, t)\} + (1-y) g_{\text{und}}(\lambda_u, t) \quad (T > 50 \text{ K}). \quad (11)$$

The spectra were thus fitted with an asymmetry function of the form given in Eq. (5) with, of course, the preliminary $g_i(t)$ replaced by the appropriate $g_p(t)$ above. The fitted parameters are a_s , a_{Ag} , y , ν_{Fe} or ν_{F} ($T < 50$ K), ν_h ($T > 50$ K), ν_d , and λ_u . Because of the rapid depolarization of the

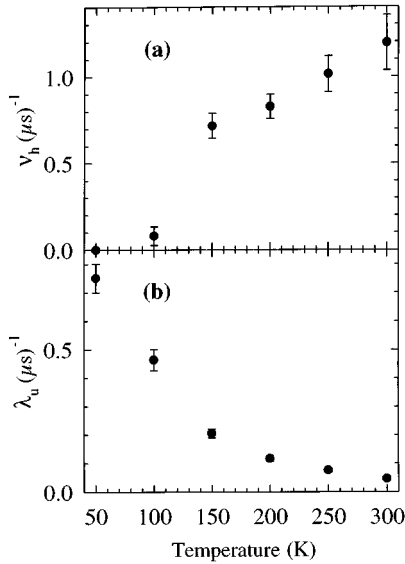


FIG. 6. Fitted values of parameters for the μSR spectra, $T \geq 50$ K: (a) ν_h , (b) λ_u .

underlying component [see Fig. 6(b)] at the lowest temperatures it becomes sufficiently similar in form to the main component that the parameter y is not well defined. In this low-temperature regime y was therefore fixed at its unvarying value at higher temperatures. Conversely at the highest temperatures the depolarization of the underlying component is slow, leading to ambiguity with the constant asymmetry from muons stopping in the silver mask. The parameter a_{Ag} was therefore fixed in the high-temperature regime at its low-temperature value. Apart from these two constraints the parameters were freely fitted. The fitted values of the $(\text{FMuF})^-$ parameter ν_d showed little systematic variation over the entire temperature range averaging at $0.22 \mu\text{s}^{-1}$, a value consistent with those reported by Brewer *et al.*¹⁰ for a range of fluorides.

Fitted values of ν_h and λ_u in the high-temperature regime are shown in Fig. 6. We comment first on the underlying component. The combination of an exponential depolarization function with a strongly temperature-dependent rate λ_u strongly suggests a dynamic process. If this is a hopping process, as is believed to be the case for the main component, then we have the possibility of hopping between two types of sites. Equations (9)–(11) would then not represent an accurate description because they imply independence of the two components. However, the fact that y and therefore the relative population of the two components apparently changes little over the 50–300 K temperature range suggests that the components are not interconnected. Beyond speculating that the value of y may be determined by implantation into different domains we do not discuss this point further and comment now on the main component. Figure 6 shows the hop rate ν_h to increase sharply above 100 K. However, the temperature dependence seems not to follow a simple Arrhenius law as the increase slows up in the region of 150 K. This may be an artefact of some imperfection in our model or it may be associated with a structural phase change at $T \geq 150$ K in $\beta\text{-(NH}_4)_2\text{FeF}_5$ reported by Calage *et al.*¹ We shall return to this point in Sec. III.

The results of fitting the low-temperature data with Eq.

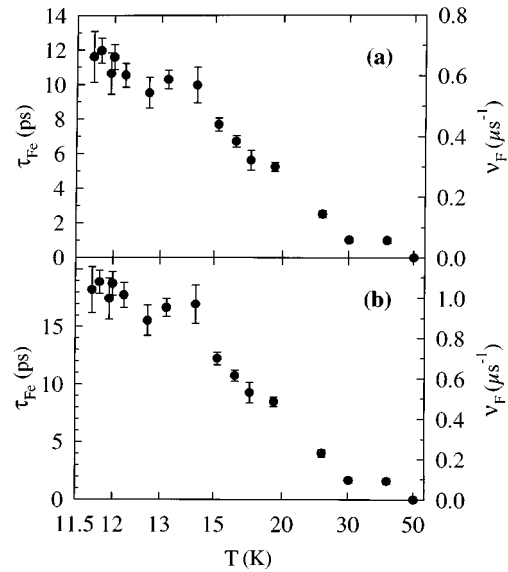


FIG. 7. Fitted values of τ_{Fe} and ν_{F} for the μSR spectra, $11.5 \leq T \leq 50$ K: (a) using the depolarization function of Eq. (10), (b) similarly but with $g_{\text{Fe-Mu}}(t)$ set equal to unity. Note that the temperature scale is nonlinear.

(10) are shown in Fig. 7(a). The ordinate here is $1/\nu_{\text{Fe}} = \tau_{\text{Fe}}$, the Fe ion spin correlation time, and equivalently the ^{19}F nuclear spin-flip rate ν_{F} . The correlation time τ_{Fe} is seen to increase with temperature decreasing towards the ordered region, as expected. It is interesting to note that if the data are fitted with Eq. (10) with $g_{\text{Fe-Mu}}(t)$ set equal to unity (i.e., turning off the direct Fe-Mu interaction) a similar plot results [Fig. 7(b)] but with the values of ν_{F} broadly increased by approximately 50%. This indicates that the indirect (Fe- ^{19}F -Mu) depolarization mechanism is somewhat stronger than the direct (Fe-Mu) one. The former type is sometimes referred to as muon-nuclear-spin double relaxation.¹⁸ In Fig. 7(b) it may be seen that ν_{F} levels off at approximately 14 K. This seems physically unlikely and the artificial cause of it may be understood by referring to Fig. 3. Increasing rate attenuates the oscillatory signal but also ultimately slows the depolarization. There is little evidence of the latter in the 30→12.5 K spectra in Fig. 1. From the fitting point of view we can therefore see that the direct Fe-Mu interaction provides an alternative depolarization channel which, by itself, would give a faster depolarization with increasing ν_{F} and decreasing ν_{Fe} and thus opposes the above slowing effect. In fact some leveling off is still evident in Fig. 7(a) and one might be tempted to try a value of Δ_{Mu} somewhat higher than our earlier estimate in order to generate a steeper rise in ν_{F} just to fall in with intuitive expectation. However, this adjustment would be rather bogus, bearing in mind that critical slowing of the Fe spins would very probably also flip the spins of nuclei contributing to the static depolarization function $g_{\text{disi}}(t) = \exp(-\lambda_e t)$. In effect this may be simulated by reducing λ_e and it was found that fitting the data with a reduced λ_e did indeed require a larger τ_{Fe} . Since we have insufficient information to pursue this point more quantitatively we settle for an analysis based on the estimated Δ_{Mu} with the depolarization function of Eq. (10) having both its basis and its limitations reasonably well understood.

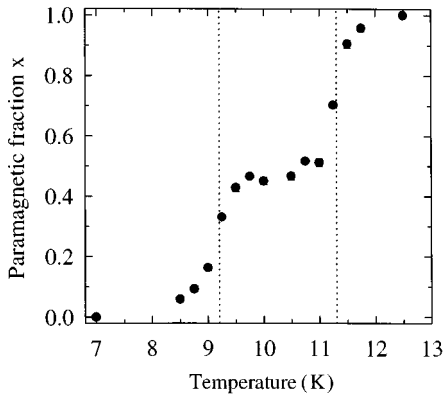


FIG. 8. Paramagnetic fraction x from the μ SR data. The broken vertical lines at 9.2 and 11.3 K are for the purpose of comparison with Fig. 12.

2. Ordering region

In the temperature range 7.0–12.5 K, which encompasses the magnetic ordering, spectra were fitted with the function

$$a(t) = a_s[xg_p(t) + (1-x)g_0(t)] + a_{Ag}, \quad (12)$$

where x is the fraction of muons in a paramagnetic environment, for which the appropriate depolarization function is $g_p(t)$. For the depolarization in an ordered environment we have taken

$$g_0(t) = \frac{1}{3} \exp(-\lambda_0 t), \quad (13)$$

where the $1/3$ factor arises from the rapid drop in initial asymmetry mentioned earlier, and the exponential form is that appropriate to the dynamic depolarization due to internal field fluctuations. The initial asymmetry is related to the paramagnetic fraction x by

$$a(0) = a_s(1 + 2x)/3 + a_{Ag} \quad (14)$$

irrespective of the particular form of $g_p(t)$ and $g_0(t)$, relying only on $g_p(t) \rightarrow 1$ and $g_0(t) \rightarrow 1/3$ as $t \rightarrow 0$. Indeed the temperature dependence of x , which is our main interest here, can be quite well extracted from the data by using some simple parametrization for $g_p(t)$. However, for consistency and to avoid introducing yet another depolarization function, we present here the results obtained using $g_p(t)$ as given in Eq. (10). To determine the temperature dependence of x with a sensible measure of its point-to-point random error, the parameters a_s , a_{Ag} , ν_d , and y were subject to the reasonable constraint that they remain constant over this small temperature range. The parameter y was fixed at its high-temperature value as before. The other three parameters were fixed by fitting simultaneously over a grid of six spectra through the range, x being taken to be 0 and 1 respectively at 7.0 and 12.5 K. With these values of a_s , a_{Ag} , and ν_d (reassuringly similar to their values in the paramagnetic region) the fifteen spectra in the 7.0–12.5 K range were individually fitted. The fitted values of λ_0 scattered around $\lambda_0 \approx 0.03 \mu\text{s}^{-1}$ with no discernible systematic trend. The fitted values of the paramagnetic fraction x are shown in Fig. 8. Clearly the ordering is segregated into two regions centred approximately on 9.2 and 11.3 K.

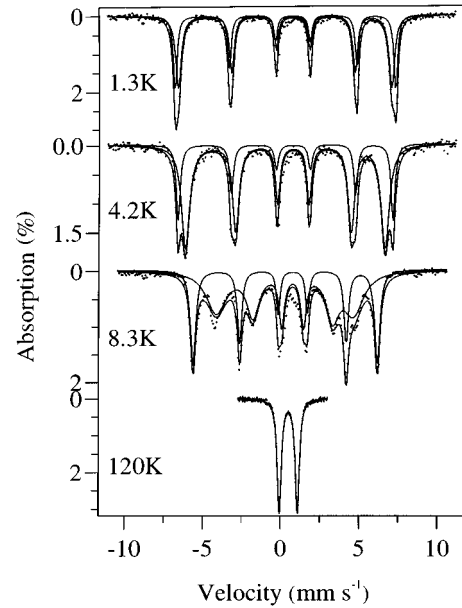


FIG. 9. Some Mössbauer spectra from β -(NH₄)₂FeF₅ at various temperatures. Fits to spectra in the antiferromagnetic phase shown here are on the basis of two discrete components.

III. MÖSSBAUER SPECTRA

A. Experiment

Absorbers were made up of approximately 20 mg cm^{-2} β -(NH₄)₂FeF₅ mixed with boron nitride. Mössbauer spectra were taken using $^{57}\text{Co}/\text{Rh}$ sources and constant-acceleration spectrometer drives operated in double-ramp mode. Three spectrometer systems were used. The first was a liquid-helium cryostat with pumping facility for temperatures of 4.2 K and below, the temperature being deduced from the measured pressure above the liquid. The second, which was used over the 5–290 K temperature range and for most of the measurements, was an Oxford Instruments continuous helium-flow cryostat controlled by an ITC4 system. In this case the sample temperature was measured separately with a carbon glass resistor incorporated into the sample holder, the calibration being accurate to better than ± 0.1 K for temperatures in the region of T_N and the stability better than ± 0.05 K. The third was a furnace equipped with a thermocouple thermometer, enabling measurements up to the decomposition temperature¹⁵ of 285 °C.

B. Analysis

Some spectra are shown in Fig. 9. The results of some fits in terms of the usual Mössbauer spectral parameters are given in Table I. These are in agreement with those of Calage *et al.*¹ It may be seen that there is little variation in the quadrupole splitting in the paramagnetic region. Calage *et al.*¹ reported that fitting of the doublet spectra required more than one component below 150 K. They attributed this to a structural phase transition and verified this with differential scanning calorimetry measurements. These showed a transition at 168 ± 1 K on heating and at 187 ± 3 K on cooling. As already remarked, such a transition may conceivably be responsible for an inflection in the temperature dependence of the muon hop rate in this temperature region. How-

TABLE I. Fitted Mössbauer spectral parameters at selected temperatures: center shift δ , quadrupole splitting ΔE_Q , quadrupole shift ε , and magnetic hyperfine field B_{hf} .

T (K)	δ (mm/s)	ΔE_Q (mm/s)	2ε (mm/s)	B_{hf} (T)	%
4.2	0.545 (3)		-0.51 (1)	42.7 (1)	26 (2)
	0.544 (2)		-0.53 (1)	39.6 (1)	74 (2)
15.7	0.547 (1)	1.086 (3)			
290	0.441 (1)	1.153 (3)			
420	0.379 (1)	1.145 (3)			

ever, although we found the fits to our Mössbauer spectra to be somewhat better with two doublet components rather than one, the difference was too small for us to draw clear conclusions about the temperature of any transition or whether the number of required components was two or more.

The basis of the fits to the antiferromagnetic spectra shown in Fig. 9 is two sextets, each modeled with a magnetic hyperfine field and a relatively small perturbing quadrupole interaction. The parameters so deduced were consistent from one sample to another except that the relative absorption in the two sextets was variable, the higher-field sextet fraction varying from 15 to 50%. A variation of this type was also noted by Calage *et al.*¹ Fitting of the spectra in this way was a useful initial parametrization and the deduced magnetization curves (B_{hf} vs T) did indeed suggest two ordering temperatures, one for each component. However, the fits at higher temperatures in the ordered region were not very satisfactory, a situation which was not convincingly improved with four components. Now in the case of $(\text{NH}_4)_2\text{FeCl}_5 \cdot \text{H}_2\text{O}$ it was found⁵ that, just below the ordering temperature, the spectral shapes could be reproduced quite well with a small number of discrete components coupled with relaxation broadening. This model was therefore tried here also. However, the fits were not quite as good and furthermore there was some inconsistency in the relative intensities of the components over the temperature range. Now although it is probable that some relaxation broadening arises in the vicinity of magnetic ordering we concluded that the principal source of broadening here was due to a distribution of magnetic hyperfine fields presumably because of some randomness in the Fe environments. Satisfactory fits were obtained with distributions $P(B_{\text{hf}})$ of hyperfine fields and examples are shown in Fig. 10. The dependence of $P(B_{\text{hf}})$ on temperature is shown in Fig. 11. It may be seen that $P(B_{\text{hf}})$ is double-peaked and also that the peaks are generally asymmetric, being skewed towards the low-field side; this latter feature is one which the other fitting models would not reproduce. As some measure of the paramagnetic fraction we take the fraction of the absorption associated with low hyperfine field, say less than 3 T. The quantity $P(B_{\text{hf}} < 3 \text{ T})$ is plotted against temperature in Fig. 12. Again, the magnetic ordering appears to be staggered with the two stages centered approximately on 9.2 and 11.3 K.

IV. DISCUSSION

A. Magnetic ordering

Both the Mössbauer and μSR experiments indicate that the ordering does not occur at a unique temperature. Further-

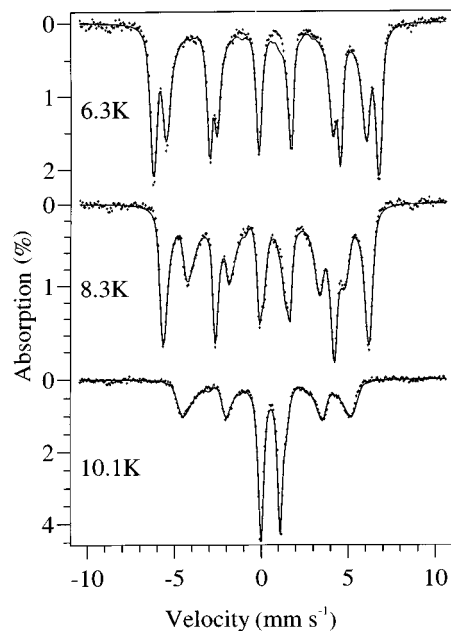


FIG. 10. Some Mössbauer spectra in the antiferromagnetic region fitted with distributions of magnetic hyperfine fields.

more the results are in very good agreement in showing the two stages in the ordering to be centered on approximately 9.2 and 11.3 K. In this respect there is some difference between our results and those of Calage *et al.*¹ in which the ordering is reported to occur just above 12 K. It seems unlikely that thermometry is responsible for this difference.

In view of the staggered nature of the ordering it is tempting to hypothesize the existence of two or more weakly coupled spin subsystems in $\beta\text{-}(\text{NH}_4)_2\text{FeF}_5$ and in $(\text{NH}_4)_2\text{FeCl}_5 \cdot \text{H}_2\text{O}$. Calage *et al.*¹ have suggested that magnetic inequivalence of Fe ions may result from differences in superexchange pathways, in turn due to different ammonium-ion orientations. It is well known that the ammonium ion can behave as a hindered rotor and indeed the pronounced temperature dependence of the quadrupole splitting in $(\text{NH}_4)_2\text{FeCl}_5 \cdot \text{H}_2\text{O}$ has been shown by Partiti *et al.*³ to be described very well by a model based on thermally activated

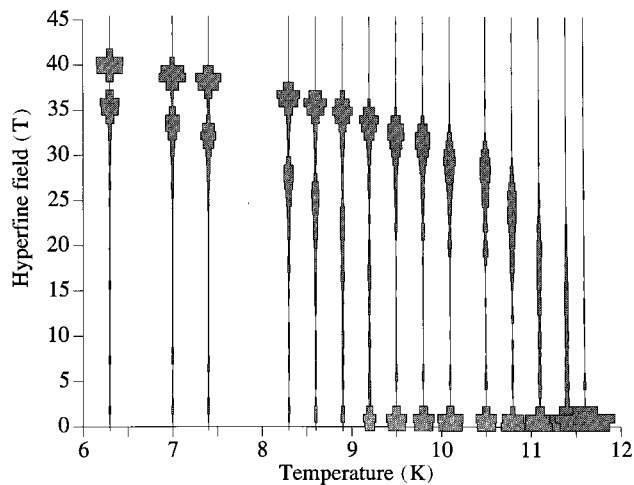


FIG. 11. Variation with temperature of the hyperfine field distributions. $P(B_{\text{hf}})$ is proportional to the width of the trace.

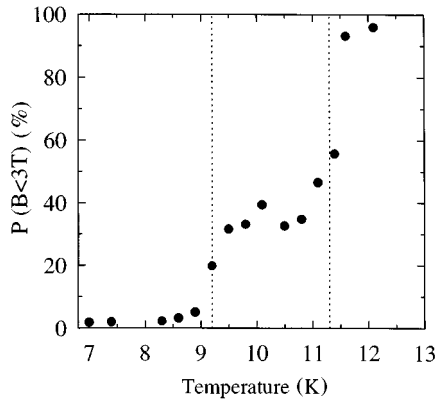


FIG. 12. Temperature dependence of the low-field fraction $P(B_{\text{hf}} < 3 \text{ T})$. Note the similarity with Fig. 8.

reorientations of the ammonium ion. The variation of the quadrupole splitting levels off below approximately 40 K presumably because the ammonium ions then have frozen-in orientations. On the other hand β -(NH₄)₂FeF₅ shows very little temperature dependence of the quadrupole splitting up to well over 400 K (Table I) so that the orientations in this case are probably determined in the preparation where the final baking is done at 383–388 K. This may be responsible for the difference discussed below between the two compounds in the relative intensities of the components of the magnetically split Mössbauer spectra.

In the case of (NH₄)₂FeCl₅·H₂O it was concluded⁵ that the antiferromagnetic Mössbauer spectra comprised a small number of discrete components, these being broadened by critical fluctuations close to the ordering region. The number of components was deduced to be either two or four, the latter being only marginally preferred on the basis of goodness of spectral fits. At about the same time Misra and Li¹⁹ reported a variable-temperature EPR study of Fe-doped (NH₄)₂InCl₅·H₂O which is isomorphous with (NH₄)₂FeCl₅·H₂O. They reported the existence of two magnetically inequivalent but crystallographically equivalent Fe ion sites. We may be fairly confident then that the antiferromagnetic Mössbauer spectra of (NH₄)₂FeCl₅·H₂O are due to two components of equal intensity. The β -(NH₄)₂FeF₅ case is clearly different. The spectral broadening has been found here to be better explained by a distribution of hyperfine fields than by relaxation effects. This points to some randomness in the Fe ion environments. Furthermore, although the distribution falls largely into two groups, the intensities of these are not generally in a 1:1 ratio but instead are variable and apparently determined in the preparation. The field distributions and mean ordering temperatures within the two groups are, however, less variable, suggesting that the Fe ion interactions are insensitive to preparation.

There are cases of materials having two transition temperatures in the temperature region of magnetic ordering but these normally involve a reconfiguration of an ordered spin system at the lower of the two temperatures. Indeed it had been earlier suggested that the lower-temperature heat-capacity cusp in (NH₄)₂FeCl₅·H₂O might be due to a spin reorientation but single-crystal Mössbauer experiments⁵ showed that the axis of Fe spin alignment remained unchanged through that temperature. In the case of

β -(NH₄)₂FeF₅ we did not have single crystals and do not know the orientation of the magnetic easy axis, but the Mössbauer and μ SR data reported here would not be explained by a spin reorientation.

It is worth noting that, in the case of two ordering temperatures, a μ SR experiment does not necessarily give a two-stage change in initial asymmetry. For a finely interwoven system it would be quite possible for all of the implanted muons to sense internal fields just below the upper of the two temperatures. A two-stage change like that observed here would require, in addition to two-stage ordering, some quirk of muon sites and field directions or the material to be effectively separated into different domains.

We conclude that the next step in the study of both (NH₄)₂FeCl₅·H₂O and β -(NH₄)₂FeF₅ would be variable-temperature x-ray and neutron diffraction. Although both compounds were confirmed by x-ray diffraction to be single phase at higher temperatures, it would be useful to know whether they remain single phase at low temperatures and also their crystallographic and magnetic structures.

B. μ SR in the paramagnetic region

The outcome of the analysis has already been given in some detail in Sec. II B so that a few summary remarks will suffice here.

The μ SR in β -(NH₄)₂FeF₅ is evidently complicated but we have been able to reproduce its principal features fairly well. Of course, our compact notation for the depolarization functions should not be allowed to obscure the fact that we have conveniently transferred to computer the pain of lengthy numerical solution. There are a number of fitting parameters and in some circumstances it has been necessary to impose constraints in order to facilitate fitting. We have declared all such cases and they are relatively few and reasonable.

Central to this analysis has been the (FMuF)⁻ depolarization function and the strong-collision model. The recognizable signal of the former has provided the means to study other interactions involving the Fe ionic spins, the ¹⁹F nuclei and the muon probe; the latter has been used to describe the effect of muon diffusion at higher temperature and to mimic the effect of ¹⁹F spin flips at low temperature. These are attributed to critical slowing down of the Fe ion spin fluctuations and the Fe-¹⁹F interaction. This indirect mechanism of muon depolarization is somewhat stronger than that of the direct Fe-Mu interaction in β -(NH₄)₂FeF₅. Measurements by ¹⁹F NMR may also be of value here, although our results for the ¹⁹F spin-lattice relaxation times (in the μ s range close to magnetic ordering) suggest that these are too small for conventional magnetic resonance. We are not able to comment on the effect of the ¹⁴N or proton spins but conventional NMR studies may possibly shed some light on the role of the NH₄ groups in the different exchange paths.

Although, at low temperature, the variation of the Fe spin correlation time (and associated ¹⁹F flip rate) is attributed to critical behavior, the staggered nature of the ordering and the limitations of our model do not allow sensible extraction of a critical exponent. We may, however, make an observation on the Fe spin correlation times τ_{Fe} shown in Fig. 7(a). At the lowest temperatures in the paramagnetic region our analysis gives $\tau_{\text{Fe}} \approx 10$ ps. Now, roughly speaking, the requirement for

noticeable critical broadening of a doublet Mössbauer spectrum is $\tau_{\text{Fe}} \approx 30$ ps. A Mössbauer spectrum taken at $T = 12$ K admits the possibility of a small line broadening, so there is no inconsistency here. A more definite statement may be made about the observation of critical behavior with the two techniques: in the Mössbauer measurements on $\beta\text{-(NH}_4\text{)}_2\text{FeF}_5$ critical effects were barely discernible at just above the upper ordering temperature; in the μSR measure-

ments on the same compound they were evident up to at least twice this temperature.

ACKNOWLEDGMENTS

We are grateful to Professor J. L. Fourquet for details of the chemical preparation and to Dr. M. P. Brown for assistance with this preparation. We also acknowledge help from several members of the ISIS staff. This work was supported in part by the EC.

-
- ¹Y. Calage, M. C. Moron, J. L. Fourquet, and F. Palacio, *J. Magn. Mater.* **98**, 79 (1991).
- ²J. N. McElearney and S. Merchant, *Inorg. Chem.* **17**, 1207 (1978).
- ³C. S. M. Partiti, H. R. Rechenberg, and J.-P. Sanchez, *J. Phys. C* **21**, 5825 (1988).
- ⁴Y. Calage, J. L. Dormann, M. C. Moron, and F. Palacio, *Hyperfine Interact.* **54**, 483 (1990).
- ⁵S. R. Brown and I. Hall, *J. Phys. Condens. Matter* **4**, 9191 (1992).
- ⁶A. Schenk, *Muon Spin Rotation Spectroscopy: Principles and Applications in Solid State Physics* (Hilger, London, 1985).
- ⁷S. F. J. Cox, *J. Phys. C* **20**, 3187 (1987).
- ⁸G. H. Eaton, M. A. Clarke-Gayther, C. A. Scott, C. N. Uden, and W. G. Williams, *Nucl. Instrum. Methods A* **342**, 319 (1994).
- ⁹We choose to refer to $(\text{FMuF})^-$ rather than $(\text{F}\mu\text{F})^-$ to signify that the muon is in a stable, bonded state.
- ¹⁰J. H. Brewer, D. R. Harshman, R. Keitel, S. R. Kreitzman, G. M. Luke, D. R. Noakes, and R. E. Turner, *Hyperfine Interact.* **32**, 677 (1986).
- ¹¹J. H. Brewer, S. R. Kreitzman, D. R. Noakes, E. J. Ansaldo, D. R. Harshman, and R. Keitel, *Phys. Rev. B* **33**, 7813 (1986).
- ¹²D. R. Noakes, E. J. Ansaldo, S. R. Kreitzman, and G. M. Luke, *J. Phys. Chem. Solids* **54**, 785 (1993).
- ¹³D. R. Noakes, E. J. Ansaldo, and G. M. Luke, *J. Appl. Phys.* **73**, 5666 (1993).
- ¹⁴U. Bentrup and L. Kolditz, *J. Therm. Anal.* **33**, 827 (1988).
- ¹⁵J. L. Fourquet, A. Le Bail, H. Duroy, and M. C. Moron, *Eur. J. Solid State Inorg. Chem.* **26**, 435 (1989); J. L. Fourquet (private communication).
- ¹⁶A. Keren, *Phys. Rev. B* **50**, 10 039 (1994).
- ¹⁷S. R. Kreitzman, R. F. Kiefl, D. R. Noakes, J. H. Brewer, and E. J. Ansaldo, *Hyperfine Interact.* **32**, 521 (1986).
- ¹⁸T. Matsuzaki, K. Nishiyama, K. Nagamine, T. Yamazaki, M. Senba, J. M. Bailey, and J. H. Brewer, *Phys. Lett. A* **123**, 91 (1987).
- ¹⁹S. K. Misra and X. Li, *Phys. Rev. B* **45**, 12 883 (1992).